Hindawi Publishing Corporation
International Journal of Rotating Machinery
Volume 2012, Article ID 321306, 12 pages
doi:10.1155/2012/321306

Research Article

Dimensionless Numerical Approaches for the Performance Prediction of Marine Waterjet Propulsion Units

Marco Altosole,[1] Giovanni Benvenuto,[1] Massimo Figari,[1] and Ugo Campora[2]

[1] *Department of Naval Architecture and Electrical Engineering, University of Genoa, 16145 Genoa, Italy*
[2] *Department of Thermal Machines, Energy and Transport Systems, University of Genoa, 16145 Genoa, Italy*

Correspondence should be addressed to Marco Altosole, altosole@unige.it

Received 2 December 2011; Revised 23 April 2012; Accepted 12 May 2012

Academic Editor: Yin Lu Julic Young

One of the key issues at early design stage of a high-speed craft is the selection and the performance prediction of the propulsion system because at this stage only few information about the vessel are available. The objective of this work is precisely to provide the designer, in the case of waterjet propelled craft, with a simple and reliable calculation tool, able to predict the waterjet working points in design and off-design conditions, allowing to investigate several propulsive options during the ship design process. In the paper two original dimensionless numerical procedures, one referred to jet units for naval applications and the other more suitable for planing boats, are presented. The first procedure is based on a generalized performance map for mixed flow pumps, derived from the analysis of several waterjet pumps by applying similitude principles of the hydraulic machines. The second approach, validated by some comparisons with current waterjet installations, is based on a complete physical approach, from which a set of non-dimensional waterjet characteristics has been drawn by the authors. The presented application examples show the validity and the degree of accuracy of the proposed methodologies for the performance evaluation of waterjet propulsion systems.

1. Introduction

The last technological advances in marine waterjets have put them ahead of conventional propeller systems for many types of high-speed marine applications, including naval vessels, ferries, workboats, and pleasure craft. Modern waterjet propulsion systems offer, for these applications, several advantages, such as high efficiency, rapid acceleration, and an excellent maneuverability, in addition to minimum possible draft with no protruding underwater appendages. This latter aspect allows operation in shallow waters and in water with floating debris that may foul or damage a typical marine propeller. This means also an increasing safety for persons and animals swimming near the vessel.

In the marine jet propulsion, a water mass is drawn into the waterjet unit through an intake screen at the base of the intake, which is mostly mounted flush with the hull bottom. The pumping unit, consisting of impeller and stator, increases the pressure of the flow, which is then discharged at high velocity at the nozzle. The reaction to this high speed jet stream provides the net thrust force, which is fully transmitted to the hull by the thrust bearing. The steering nozzle directs the jet stream as commanded by the helm, providing high turning forces to either port or starboard. An independent reverse deflector, usually hydraulically actuated, directs the jet stream back under the hull to provide powerful astern thrust.

Although the waterjet plants are nowadays more and more used for the propulsion of fast ships, there is not yet a consolidated theory or methodology able to help the naval architect or the marine engineer in an early design stage. On the contrary, in the pertinent literature, it is possible to find out specialized studies concerning different aspects of the waterjet propulsion.

A brief analysis of the papers presented at several international conferences [1–14] shows that the developed researches follow, in general, two different approaches, as noted in [15]:

(i) the detailed prediction of hydrodynamic behavior and
(ii) the use of numerical modeling strategies for the integration of waterjets into propulsion system designs.

The first approach has recently received a major boost from the use of computational fluid dynamics (CFD) to optimize specific components of the waterjet system, such as pump impeller or inlet duct [1–6]. Moreover CFD calculations are claimed a reliable tool in predicting both noncavitating and cavitating conditions. However the main drawback of the method is that it does not allow the system designer to explore the full range of design options for different numbers of waterjets of different sizes [15]. In other words, CFD methods are useful to optimize propulsive solutions already defined for specific applications.

On the other hand, the second approach is more useful to carry out the propulsion system studies necessary in order to assess the feasibility of different powering solutions and especially to allow the power and propulsion system to be matched to the ship operating profile. In this context, it is worthy to mention the significant contributions of Van Terwisga [7, 8], MacPherson [9], and Allison [10], directed to develop parametric models able to take into account the effect of waterjet-hull interaction on thrust and propulsive efficiency. Obviously the reliability of these methods is conditioned by the availability of design information. Another limitation of the approach proposed by [9] is its poor ability to predict the onset of pump cavitation.

In addition to those mentioned before, there are also other methods developed to analyze the maneuvering capabilities of the vessels. Virtual simulation of ship propelled with waterjets became important for the optimization of the dynamic characteristics of the propulsion and to set the propulsion controller strategies [11–14]. Also this technique requires the knowledge of design information concerning the waterjet system.

Returning now to the aims and motivations of this work, as stated before, there is not yet a consolidated methodology able to help the naval architect or the marine engineer to solve the practical problem of selecting the most appropriate waterjet for a specific application. Very often indeed the ship designer does not have other chance than to rely on the experience of the waterjet manufacturers.

In general, for the selection of the proper waterjet unit in combination with a certain hull, the waterjet manufacturers usually provide a diagram showing the effective thrust, as function of craft speed and engine brake power; the term "effective thrust" means the jet thrust which can be directly compared with the hull resistance of the ship (interesting information about the correlation factor between jet thrust and hull resistance can be found in [16]). Therefore, on the same diagram, jet thrust and hull resistance are superimposed, and cavitation limit is also reported. On this basis the naval architect is able to check if the available jet thrust is adequate to meet the ship resistance demand and to avoid the risk of cavitation.

The present study aims to satisfy the aforementioned requirement to offer the designer a tool to evaluate, in a preliminary way but with sufficient accuracy, the type of waterjet to be used and its performance, without the help of the manufacturers, usually available to give only very limited information, because of obvious market reasons.

In order to reach this objective, two nondimensional numerical approaches, one referred to jet units for naval applications and the other more suitable for planing boats, are presented and discussed in the following sections.

The developed procedures, prepared on the basis of an extensive collection of information about the performance of current waterjets, can represent, in authors' opinion, a useful tool for the ship designer in order to predict the waterjet working points in design and off-design conditions and to investigate several propulsive options during the ship design process.

2. Waterjet Performance Maps

Waterjet cavitation information is traditionally provided in accordance with two typical design strategies, followed by the main jets manufactures and based on the possibility for the naval architect to select the best impeller for a certain jet model. For instance, in Figure 1, a jet performance prediction, referred to a particular impeller, is shown in terms of thrust (on the left of the figure) and rotational speed (on the right); in this kind of representation, the two cavitation lines show two cavitation levels, that is, the lower limit, which is referred to the cavitation inception of the pump, and the heavier cavitation limit. In fact, these two lines subdivide the jet working area in three zones, as illustrated in Figure 1 on the basis of the scheme adopted by Kamewa-Roll Royce; the first zone (indicated as "unlimited") is free from cavitation, the second one is characterized by a time working limit lower than 500 hours per year (that means a presence of the cavitation phenomena in a moderate form), and the third zone, with a time-working limit lower than 50 hours per year, then characterized by strong cavitation phenomena.

On the contrary, in the jet performance prediction of Figure 2, the several cavitation lines (dashed lines) are referred to several impeller options, for which the corresponding jet power absorption curves, according to a cubic law with the impeller speed, are reported on the right of the same figure. In fact, an impeller can be tuned to optimize the rotational speed by trimming the trailing edge of each blade, that is, modifying the blade pitch. This has the effect of trading torque for rpm at similar power absorption. Then, for the same jet model, several impeller types, having same diameter but different blade pitch, can be used. Obviously, a different value of the blade pitch (corresponding to a different impeller type) entails a different cavitation limit and a different power/rpm curve, as it is, respectively, shown on the left and on the right diagrams of Figure 2. In particular, each impeller type is usually defined by a number representing the power absorption in kilowatts (kW) at a precise rotational speed, taken as a reference (according to "Hamilton Jet" or "Ultrajet" nomenclature, the reference speed of the impeller is 1000 rpm, so, for instance, impeller "Type 48" means that the pump absorbs 48 kW at 1000 rpm).

In the case of larger marine waterjets, to be used for ships applications, the jet manufacturer usually optimizes the impeller geometry mainly from an hydrodynamic point of view, without showing to the naval architect the several

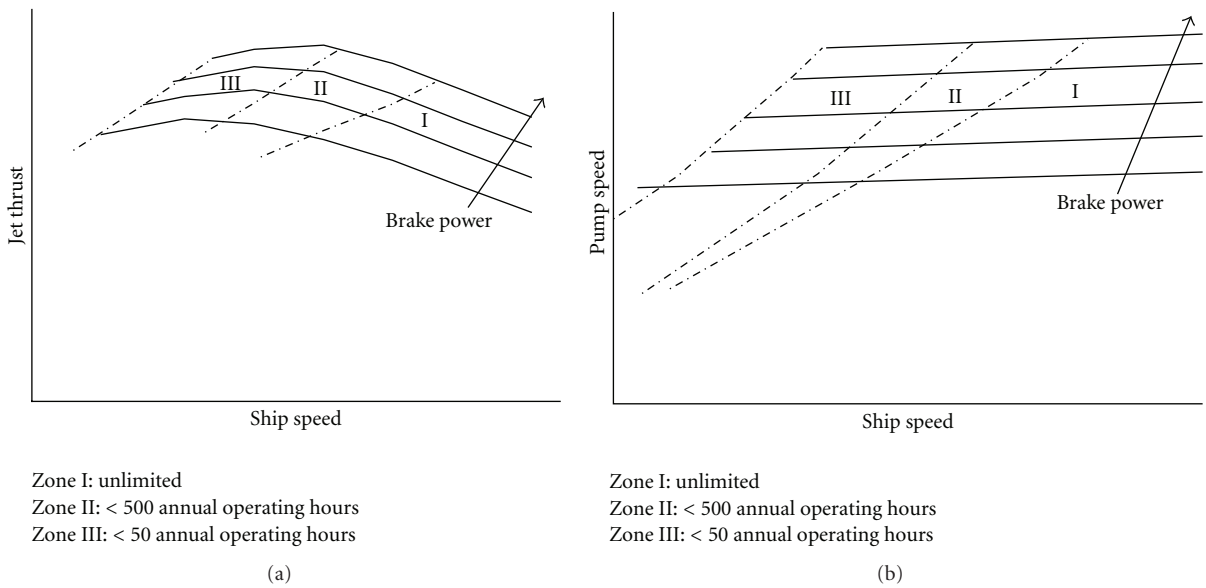

Zone I: unlimited
Zone II: < 500 annual operating hours
Zone III: < 50 annual operating hours

(a)

Zone I: unlimited
Zone II: < 500 annual operating hours
Zone III: < 50 annual operating hours

(b)

Figure 1: Typical jet curves ("Kamewa-Roll Royce" representation).

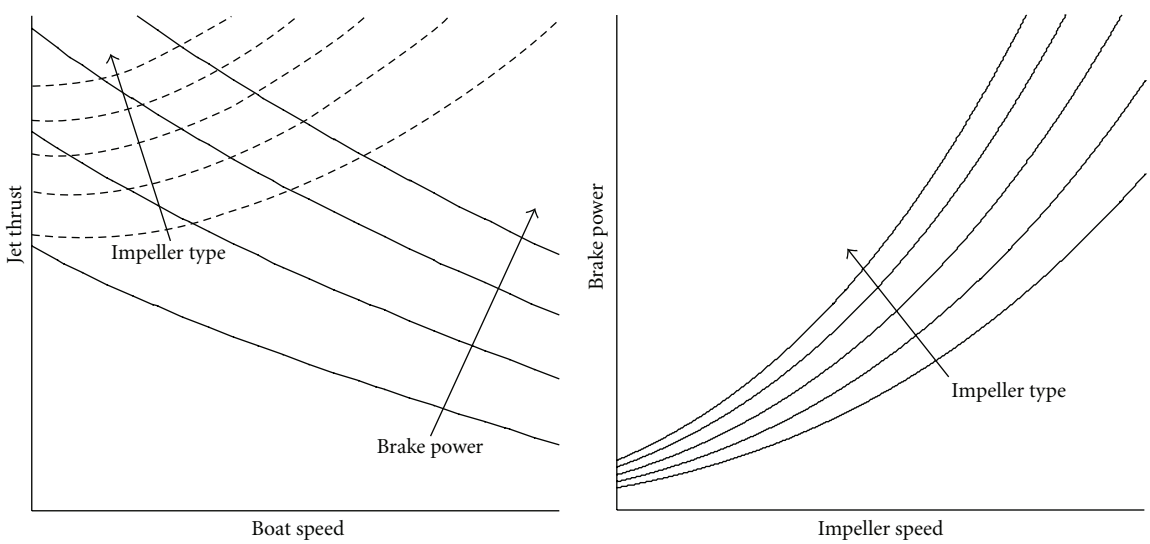

(a)

(b)

Figure 2: Typical jet curves ("Hamilton Jet" representation).

possible types of impeller to be mounted on the same jet model. This design procedure means that once the impeller pitch is selected, the rotational speed is also fixed at the considered power; therefore, the gear ratio, due to the particular adopted engine, is a fixed choice too. It has to be noted that for a ship propulsion system, the gearbox is traditionally designed individually, on the contrary, in the case of smaller planing craft applications, the naval architect can select the proper gear ratio among several options, because of the large production of these smaller gearboxes. This important difference between ship and boat applications, regarding gear ratio selection, entails the two different jet performance prediction representations, shown in Figures 1 and 2. Summarizing, manufacturers of larger jet models usually provide the final performance prediction, yet referred to the best possible impeller, while manufacturers of smaller waterjets usually give a performance prediction showing several impeller options, to be adopted for the same jet model.

3. Numerical Approaches to Jet Powering Prediction

Although several design methods have been published over the years, there is not yet a consolidated theory or methodology able to help the naval architect or the marine engineer to

select the proper existing waterjet for a defined application. The common practice of ship designers is to refer to the jet manufacturers for the selection of the waterjet size, with the obvious advantage of the accuracy of results but usually limited to a precise propulsion plant configuration and to a defined design condition. A much better possibility could be the availability of a reliable and simple calculation procedure, able to foresee the waterjet working points in design and off-design conditions, representing in this way a useful step forward for the naval architect and the marine engineer.

In the following sections, two nondimensional numerical approaches are illustrated, one referred to naval applications and the other to planing boats, in order to offer to the designer clear and simple general tools for the choice of the best waterjet size and the evaluation of its performance.

3.1. "Generalized Map" Method. A waterjet propulsion system is characterized mainly by the kind of impellers adopted. Many types of pumps have been used, such as centrifugal, mixed flow-mainly radial, mixed flow-mainly axial, and purely axial flow pumps.

It is well known that for axial pumps the efficiency is typically less than for mixed flow pumps [17–19]. For this reason, mixed flow pumps are the most used in the waterjet propulsion plants, while axial pumps are used mainly for waterjet propulsion in very high-speed applications, due to their lower size and weight. A typical mixed flow pump for waterjet propulsion is shown in Figure 3.

The dynamic similarity theory [17–19] allows the pump design on the basis of experiments on a scale model, characterized by dimensions less than full size. The performance of the full size pump can be drawn from that of the model by means of suitable scale factors. This is true at design and, with good approximation, off-design working conditions.

In a previous paper [20] the authors have superimposed for comparison the performance maps of two different mixed flow pumps of the FPI society [21], characterized by a maximum impeller diameter of 16″ and 42″, respectively (Figure 4). The superimposition is made possible, in spite of the very different characteristics of the two pumps (head, volumetric flow rate, rotational speed, etc.), by presenting the maps in nondimensional form, that is dividing each variable reported in the figure for the respective value referred to the pump design condition. The two considered pumps have the same numerical value of the specific speed ($n_s = 182$ [rpm m$^{3/4}$ s$^{-1/2}$]), defined by

$$n_s = n\frac{\sqrt{Q}}{\sqrt[4]{H^3}}. \tag{1}$$

The comparison reported in Figure 4 shows an almost perfect superimposition between the two considered performance maps, in terms of both constant speed curves and constant efficiency curves.

The conclusion that different turbomachines, having the same geometrical configuration (mixed flow, axial flow, etc.) and the same (or near) specific speed, are characterized by the same (or near) performance maps, if reported in nondimensional form, is confirmed also in [22], where substantial analogies are verified in the performance maps of various pumps, used for waterjet propulsion, even if not designed in strictly dynamic similarity.

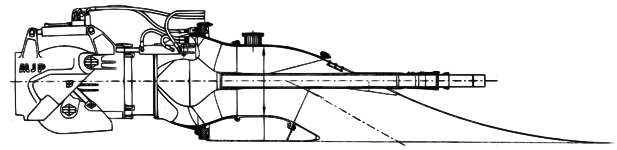

Figure 3: Typical waterjet with mixed-flow pump.

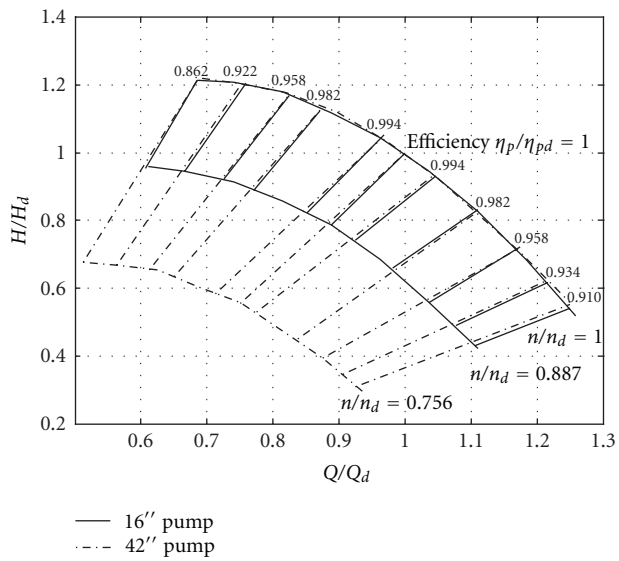

Figure 4: Comparison between performance maps of two different mixed-flow pumps.

A further confirmation follows from the comparison reported in Figure 5, where nondimensional performance maps of two axial flow pumps, both used for waterjet propulsion, are superimposed [20].

Despite the two pumps of Figure 5 are presumably not designed in dynamic similarity (n_s of SJ 6-1 pump is 75.31 while n_s of FT 12-1 pump is 63.42), the respective nondimensional constant speed and constant efficiency curves are characterized by similar pattern and consecutive disposition (with the only exception of the .955 efficiency curve of the FT 12-1 pump).

On the basis of the good agreement found in the previous comparisons, the authors decided to generate a generalized nondimensional performance map for single-stage pumps.

As pointed out, pumps of the mixed flow type are adopted in the majority of the waterjet propulsion applications. Therefore, a significant example of this type of pumps has been chosen as a starting base for the generation of the generalized pump map. The selected pump, for which a sufficient documentation in terms of characteristic curves was available, is the mixed flow pump: C 1PPA 155. This pump is designed specifically for waterjet propulsion by TM.P. S.p.A. [23], and it is characterized by a specific speed $n_s = 123$.

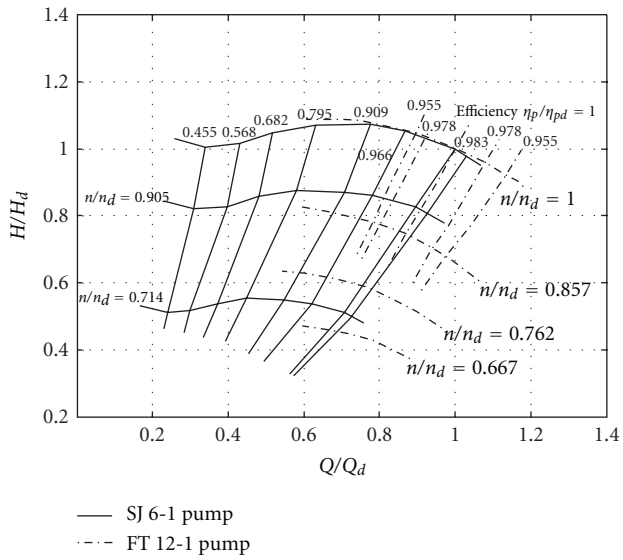

Figure 5: Comparison between performance maps of two axial-flow pumps.

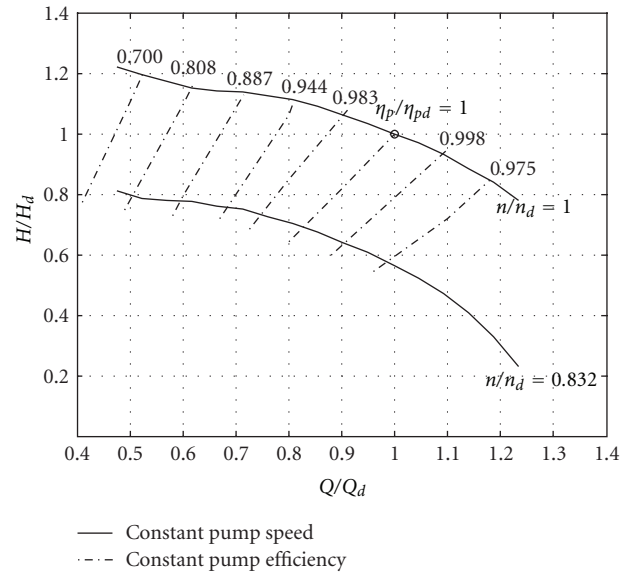

Figure 6: "Termomeccanica C 1PPA 155" pump performance map.

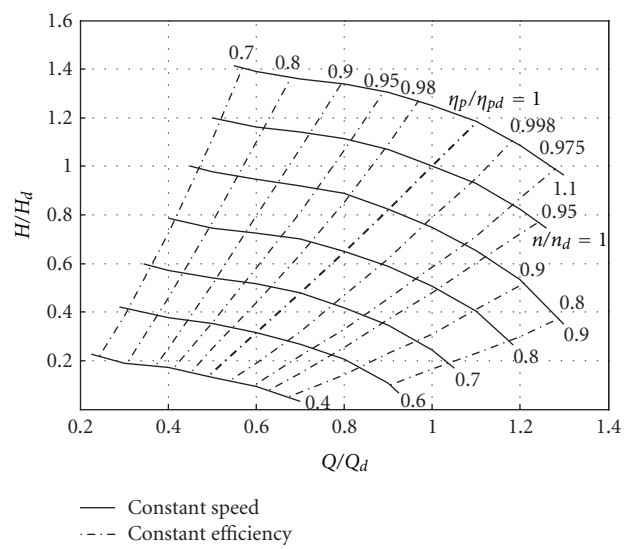

Figure 7: Generalized mixed-flow pump performance map.

The performance map of the pump C 1PPA 15 is given in Figure 6, showing, in nondimensional form, the available constant speed curves in the head-flow rate plane. In the same figure, the pump efficiency is reported for different working condition at the design speed.

The generalized mixed-flow pump performance map, reported in nondimensional form in Figure 7, has been obtained starting from the performance data of the above mentioned pump. In particular, the constant speed curve, referred to the design condition ($n/n_d = 1$ in Figure 7), is the same curve reported in Figure 6. While the other off-design constant speed curves, in Figure 7, are generated starting from $n/n_d = 1$ to $n/n_d = .832$ constant speed curves of Figure 6, by applying the similarity concepts discussed before and considering the analogies observed, for the same curves, in the pump maps of Figures 4 and 5.

Analogous considerations and procedures may be applied also to the generation of the constant efficiency curves in the map of Figure 7.

It should be noted that the reference specific speed of the generalized pump performance map of Figure 7 ($n_s = 123$) is the same of the pump whose characteristic curves were used as starting base for the map generation.

However, as demonstrated by the authors in [20], if the dynamic similarity law is observed (mainly as regards the specific speed equality or near equality), the concept of a generalized nondimensional map, as shown in Figure 7 for mixed-flow impellers, can be applied to a large number of pumps of different size. Analogous considerations and procedures may be applied also to the generation of the constant efficiency curves in the map of Figure 7.

By using the proposed generalized pump performance map, it is possible to obtain in an easy way the pump characteristic curves (in the head-flow rate plane) for the specific application. This information is required to calculate the waterjet thrust as function of ship speed and engine power by means of the simple procedure described hereinafter.

As known, the waterjet propulsion is based on the action-reaction principle, a mass of sea water enters through the inlet system, energy is added to the flow by the pump, and the water is accelerated and ejected at high velocity through the exit nozzle. The change in momentum of the water entering and leaving the waterjet system produces the thrust for the propulsion of the ship. Then the thrust T_{wj} produced by the waterjet system is expressed as follows:

$$T_{\mathrm{wj}} = \rho Q\left(V_j - V_a\right). \tag{2}$$

The jet velocity V_j is related to the jet nozzle area A_j as follows:

$$V_j = \frac{Q}{A_j} \tag{3}$$

while the approaching velocity V_a can be calculated as

$$V_a = \frac{V}{[1 + (V/(a+1))(\delta l_i/Q)]}, \tag{4}$$

where further information about the coefficient a and the thickness δ of the boundary layer can be found in [16, 24].

The pump power demand to the prime mover (usually a high speed diesel engine) can be obtained from the pump hydraulic power, taking into account the pump efficiency η_p, the relative rotative efficiency η_r and the mechanical efficiency η_m, as follows:

$$P_B = \rho g \frac{QH}{\eta_p \eta_r \eta_m}, \tag{5}$$

where the head H required by the pump is calculated as

$$H = \frac{Q^2}{2g\eta_N A_j^2} - (1-\zeta)\frac{V_a^2}{2g} + h_j, \tag{6}$$

ζ and h_j being, respectively, the inlet duct loss coefficient and the height of jet centerline above sea level.

The curve of the head required (as function of Q), expressed by the above equation, has to be compared with the head provided by the pump, obtained by means of the generalized pump map introduced before. From the equilibrium condition, it is possible to find the relation between ship speed and flow rate for each pump speed, and thus to calculate the jet thrust by (2).

In order to consider the influence of cavitation phenomena on the pump performance, in the numerical model, the pump head and efficiency values, provided by the proposed map, are properly corrected.

Two simple equations are adopted for the corrections, the first one for the head (H) correction

$$H_{\text{corr}} = H\left(1 - \frac{1 - F_{\text{corr}}}{1.35}\right) \tag{7}$$

and the second one for the pump efficiency (η_p) correction

$$\eta_{p\,\text{corr}} = \eta_p F_{\text{corr}}. \tag{8}$$

The pump head and efficiency correction function (F_{corr}) is reported in Figure 8, depending on the suction specific speed of the pump (n_{ss}). In fact, the latter parameter is a significant cavitation index, used to discriminate cavitating conditions from non-cavitating ones [9] as follows:

$$n_{ss} = n\frac{Q^{1/2}}{(g\text{NPSH})^{3/4}}, \tag{9}$$

where NPSH is the net positive suction head as follows:

$$\text{NPSH} = \frac{(p_a - p_v)}{\rho g} + (1-\zeta)\frac{V_a^2}{2g} - h_j. \tag{10}$$

The correction function and (7) and (8) are generated simultaneously in a trial and error procedure. This procedure has the objective of obtaining the best fitting of the reference thrust and constant pump speed curves, at constant power, provided by the waterjet manufacturer in the manner of Figure 1.

It must be observed that the presented pump head and efficiency corrections apply only when the pump works in cavitation conditions, that is, in the zones II and III of Figure 1.

3.2. "Nondimensional Jet Curves" Method. A successfu numerical approach should be based on simple and clearly defined parameters and should be applicable to a large range of waterjets sizes. A set of general waterjet performance curves that meets these criteria is herein proposed in analogy with the well-known marine propeller series.

All of the thrust curves relative to a defined waterjet commercial model for planing crafts can be collapsed into a thrust coefficient $K_{T_{\text{wj}}}$ depending on torque α (or $K_{Q_{\text{wj}}}$) and advance J_{wj} coefficients as

$$K_{T_{\text{wj}}} = \frac{T_{\text{wj}}}{\rho n^2 D_i^4}, \tag{11}$$

$$\alpha = \frac{C}{\rho D_i^5} \text{ or the equivalent torque coefficient,}$$
$$K_{Q_{\text{wj}}} = \frac{Q_{\text{wj}}}{\rho n^2 D_i^5} = \frac{\alpha}{2\pi}, \tag{12}$$

$$J_{\text{wj}} = \frac{V}{nD_i}. \tag{13}$$

The thrust cavitation limits, each corresponding to a different constant value of α, can be also collapsed into a cavitation thrust coefficient $\tau_{C_{\text{wj}}}$ depending on cavitation number σ_{wj} as

$$\tau_{C_{\text{wj}}} = \frac{T_{\text{cav}}}{\rho A_i V^2},$$
$$\sigma_{\text{wj}} = \frac{p_a - p_v}{\rho V^2}. \tag{14}$$

The same traditional definitions used for propellers have been utilized as far as possible, in order to make the method much more user-friendly for the propulsion boat designer.

Once computed all of these coefficients through several performance maps of many commercial waterjets, the $K_{T_{\text{wj}}}$ and $\tau_{C_{\text{wj}}}$ trends have been determined by using a proper fitting technique. As an example, the computed thrust coefficients $K_{T_{\text{wj}}}$ and $\tau_{C_{\text{wj}}}$, respectively, versus the advance coefficient J_{wj} and the cavitation number σ_{wj}, are compared with the determined fitted curves in Figures 9 and 10. It has to be pointed out that the trends shown in these figures for the two thrust coefficients correspond to the same constant value of the torque coefficient α.

The entire set of curves for the coefficients of the waterjet series so established, for different values of α, is presented in Figures 11 and 12.

In comparison with screw propellers, the thrust coefficient curve for a waterjet is much more flat, while the torque

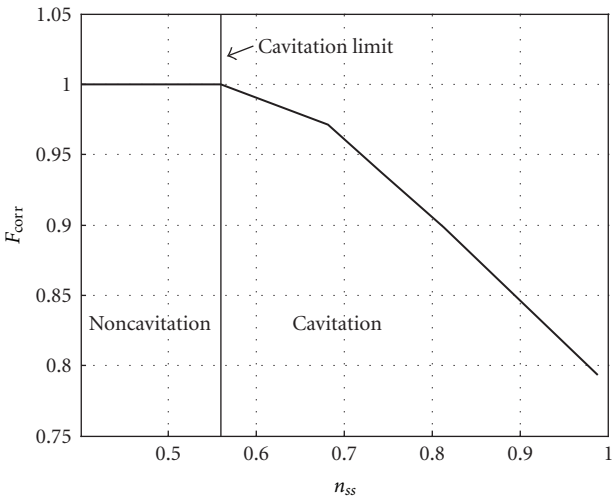

Figure 8: Correction function for pump cavitation.

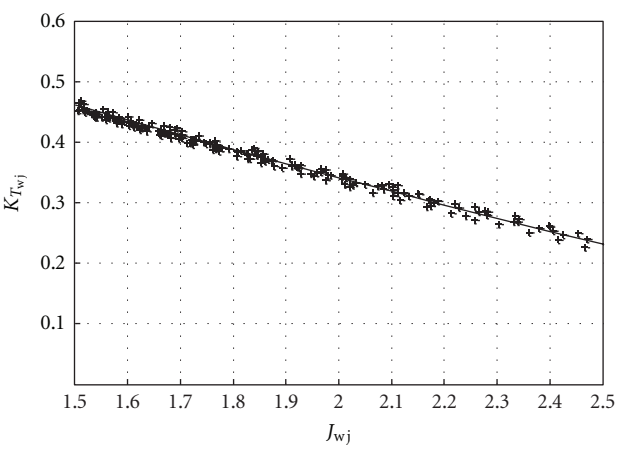

Figure 9: $K_{T_{wj}}$ curve fitting.

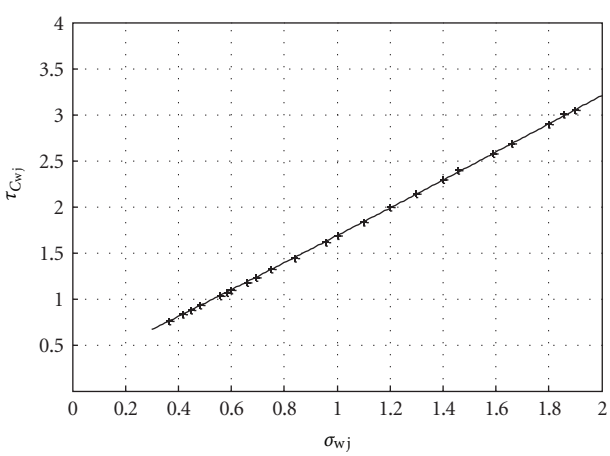

Figure 10: $\tau_{C_{wj}}$ curve fitting.

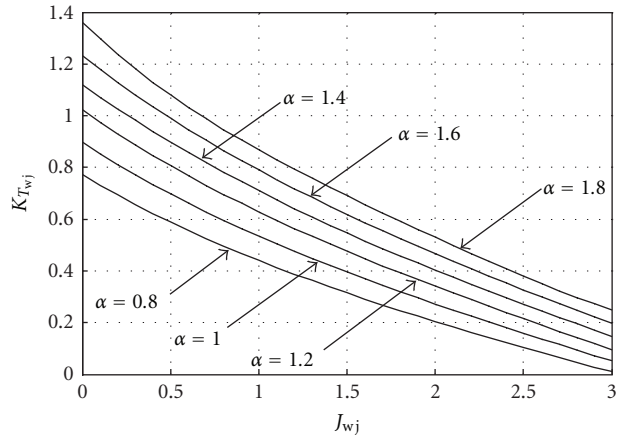

Figure 11: Jet thrust coefficients.

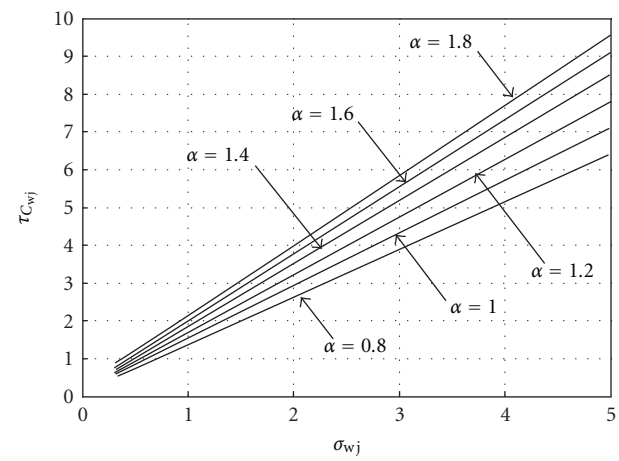

Figure 12: Cavitation coefficients.

coefficient is assumed quite constant. This means that the influence of ship's speed on thrust and torque is much less pronounced for a waterjet than for a screw propeller. The reason for this behavior is that the approaching velocity V_a in correspondence of the waterjet inlet, because of the waterjet pump location relative to the hull, is surely affected by the ship's speed but is much more determined by the impeller speed [25].

The waterjet performance prediction technique developed in this paper is similar to the calculation procedure for speed-power prediction of the propeller. Most waterjet characteristics, in fact, are reported in the form of $K_{T_{wj}}$, $K_{Q_{wj}}$ versus J_{wj}. The effort required to have this familiar format for naval architects also in waterjet propulsion design is compensated by computation time reduction in predicting jet performance and optimizing propulsion system.

Selecting a best waterjet model to satisfy the craft thrust requirements leads to reformatting jet characteristic data on the basis of the ratio $K_{T_{wj}}/J_{wj}^2$ in analogy with the propeller case, in order to eliminate the unknown variable rpm from the early prediction calculations.

For each waterjet unit, starting from (11) and (13), the following relation is obtained:

$$\frac{K_{T_{\mathrm{wj}}}}{J_{\mathrm{wj}}^2} = \frac{T_{\mathrm{wj}}}{\rho D_i^2 V^2}. \tag{15}$$

Assuming that each waterjet unit produces equal thrust for a multijet craft, the thrust required by each waterjet to satisfy the hull resistance would be

$$T_{\mathrm{wj}} = \frac{R_T}{(1-t)N_{\mathrm{wj}}}. \tag{16}$$

Equating the thrust provided by waterjets to the thrust required by the hull

$$\frac{K_{T_{\mathrm{wj}}}}{J_{\mathrm{wj}}^2} = \frac{R_T}{\rho(1-t)D_i^2 V^2 N_{\mathrm{wj}}}. \tag{17}$$

In this way, for each craft velocity, a quadratic relation between $K_{T_{\mathrm{wj}}}$ and J_{wj}, representing the ship resistance, is obtained.

Once the number of jets N_{wj} has been established, the only significant variable that can influence $K_{T_{\mathrm{wj}}}/J_{\mathrm{wj}}^2$ is the impeller diameter D_i.

Selecting impeller diameter and so the commercial waterjet model size is important not only for geometric constraints of craft operation and installation, but also for thrust loading and cavitation considerations. Since the variable $K_{T_{\mathrm{wj}}}/J_{\mathrm{wj}}^2$ is mainly a function of impeller diameter and craft velocity, the diameter, if other design constraints permit, should be selected at the design craft speed ensuring a value of $K_{T_{\mathrm{wj}}}/J_{\mathrm{wj}}^2$ for which the best waterjet efficiency is reached. As shown in Figure 13, the peak jet efficiency is attained for $K_{T_{\mathrm{wj}}}/J_{\mathrm{wj}}^2 = 0.18$. This value could be a good point of reference for the selection of the impeller diameter and so of the available waterjet unit size.

Waterjets manufacturers usually provide several impellers of different ratings to be matched with engines directly or through available gearboxes. As previously mentioned, the power absorbed by the pump as function of the rotational speed follows approximately a cubic law. For the same commercial jet model, it is possible to obtain from manufacturers several cubic laws, that is, several C coefficients (impeller rating), by adjusting, for instance, the pitch of impeller blades. At present, the impeller ratings for a commercial waterjet model may vary in the range: $0.8 \le \alpha \le 1.8$.

This means that, for the same input power, the corresponding waterjet rpm can vary between two values (see Figure 14, where the Power/Rpm range is shown for three different impeller diameters). The impeller rating should be usually selected within this range in order to lower the possible rpm and to improve the cavitation margins. On the other hand, it is possible to use reduction gearboxes in order to reach the required power at lower engine speed but with consequential extra cost, weight, and efficiency losses.

Once determined the impeller rating (coefficient α), it is possible to draw for each craft speed the corresponding quadratic relation between $K_{T_{\mathrm{wj}}}$ and J_{wj} representing the boat's resistance in the $K_{T_{\mathrm{wj}}}$ diagram. The intersection with the offered $K_{T_{\mathrm{wj}}}$ curve gives the operational point of the waterjet J_{wj}. Then from the equilibrium operational points J_{wj}, it is possible to determine the waterjet shaft speeds for the different craft speeds and so the provided waterjet thrusts.

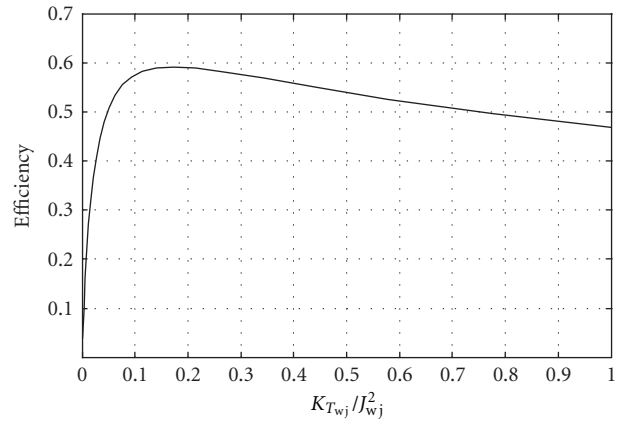

Figure 13: Waterjet efficiency versus $K_{T_{\mathrm{wj}}}/J_{\mathrm{wj}}{}^2$.

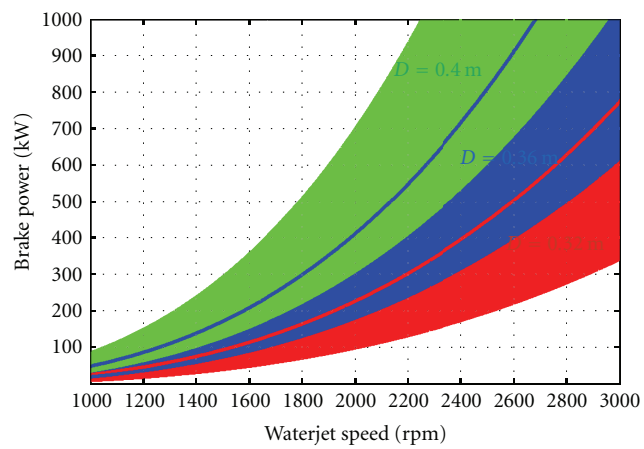

Figure 14: Power/RPM curves.

It is worthy to note that, in case of marine propeller propulsion, the power load curve is a cubic law only if the craft resistance is a quadratic curve of velocity. Only in these particular circumstances, in fact, the operational points in the propeller open water diagrams are always the same, and so there is a linear relation between V and rpm in the entire propeller working area. On the contrary, in case of waterjet propulsion, the power load curve is considered as a cubic law because of assumed hypotheses [25], for both a square resistance curve (V linear with rpm) and a planing craft resistance curve (V not linear with rpm).

In order to check if the so-calculated waterjet operational points are below the cavitation limit, it is sufficient to determine the corresponding cavitation thrusts by means of the coefficient $\tau_{C_{\mathrm{wj}}}$ curve corresponding to the selected impeller rating α.

The design process to obtain the matching between craft hull and waterjet thrust for a given craft speed can be

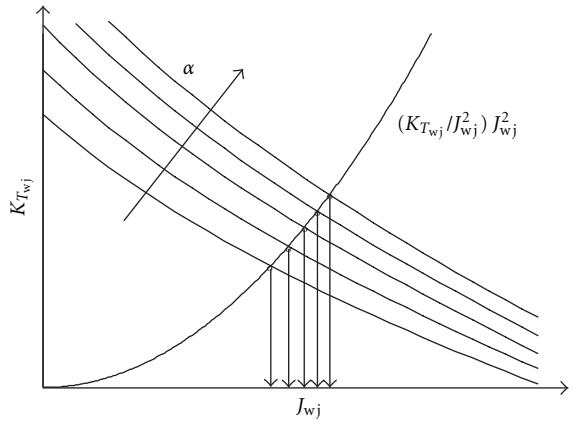

Figure 15: $K_{T_{wj}}$ curves matching.

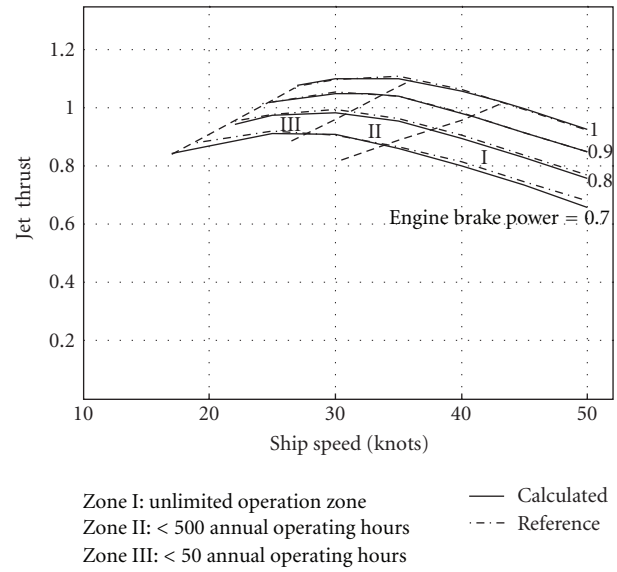

Figure 16: Thrust versus ship speed waterjet map.

summarized as follows.

(1) Select the impeller diameter on the base of arrangement criteria or calculate the optimum impeller diameter from the best-efficiency point of view ($K_{T_{wj}}/J_{wj}^2 = 0.18$).

(2) Find, for every value of α, the advance coefficients J_{wj} corresponding to the crossing points between the $K_{T_{wj}}$ curve and the dimensionless resistance curve $(K_{T_{wj}}/J_{wj}^2)J_{wj}^2$ as it is illustrated in Figure 15.

(3) Calculate the waterjet speed n required to reach the design velocity V from the value of J_{wj}.

(4) Calculate the waterjet thrust T_{wj}.

(5) Calculate σ_{wj} for the design velocity and find the corresponding value of $\tau_{C_{wj}}$ for every α.

(6) Calculate the waterjet cavitation thrust.

(7) Select the proper value of α in accordance with the available gear ratio and cavitation limit.

(8) Calculate the waterjet power required by means of $P_B = \alpha\rho D_i^5 n^3$.

In order to have a better agreement of the obtained results with the data of the most jet manufacturers present on the market, the following empirical correction, able to take into account different impellers sizes and efficiencies, is suggested to be applied to the final value of the jet thrust:

$$T_{\text{wj corrected}} = T_{\text{wj}}(D_i + 0.64)^{0.4}(0.0073V + 0.8625). \quad (18)$$

For the same reason, the thrust cavitation limit may be corrected as

$$T_{\text{cav corrected}} = T_{\text{cav}}(1.36 - D_i)^{0.6}. \quad (19)$$

These corrections, proposed by the authors, have been empirically determined on the basis of the current jet performance predictions provided by several manufacturers. They mainly depend on the impeller diameter D_i, that is, the variable most representative of the pump efficiency.

4. Results and Validation

In order to test the proposed numerical procedures, three waterjet propulsion applications are considered in the following. The first is referred to a large Kamewa waterjet, whose performance map is derived by using the dimensionless pump map of Figure 7. Instead the second and the third applications are referred to two smaller waterjets, characterized by almost the same impeller diameter, but produced by different manufactures, Hamilton Jet and MJP. The thrust curves of the last two jet models have been selected by the authors to validate the numerical method based on the dimensionless jet coefficients.

4.1. Case Study 1. In order to show the possible use and the effectiveness of the proposed performance map, the developed methodology is applied to the waterjet "Kamewa 200 SII," whose design power range is 16 ÷ 24 MW.

The comparison between jet manufacturer data (dashed and dotted lines) and calculations (continuous lines) is illustrated in Figures 16 and 17, where the jet thrust curves and the pump speed curves versus ship speed are shown for different engine power values. As it can be seen in Figure 16, the thrust curves at constant power present a decreasing slope when the ship speed decreases. This behavior is mainly due to the pump cavitation phenomena.

The good results of the comparison between the calculated and manufacturer data, in the noncavitation zone (zone I), are due mainly to the pump performance map characteristics. This fact confirms the validity in this application of the presented generalized pump performance map. This is the most important result of the proposed validation.

The good results of the comparisons relative to the pump working in cavitation conditions (II and III zones in Figures 16 and 17) demonstrate a good matching between the generalized pump performance map and the cavitation correction factor.

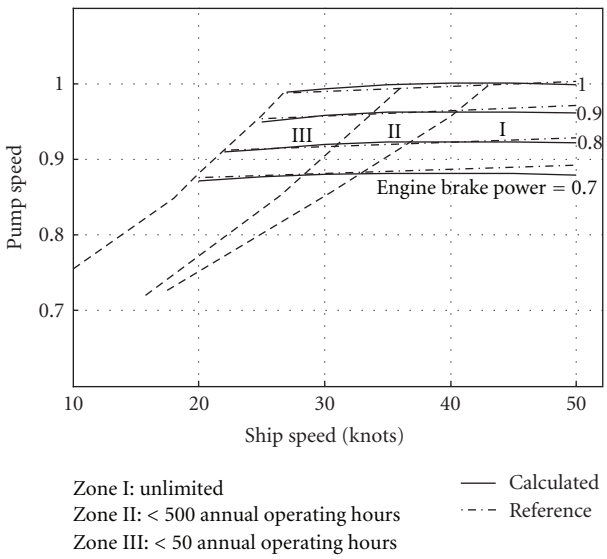

Figure 17: Pump speed versus ship speed waterjet map.

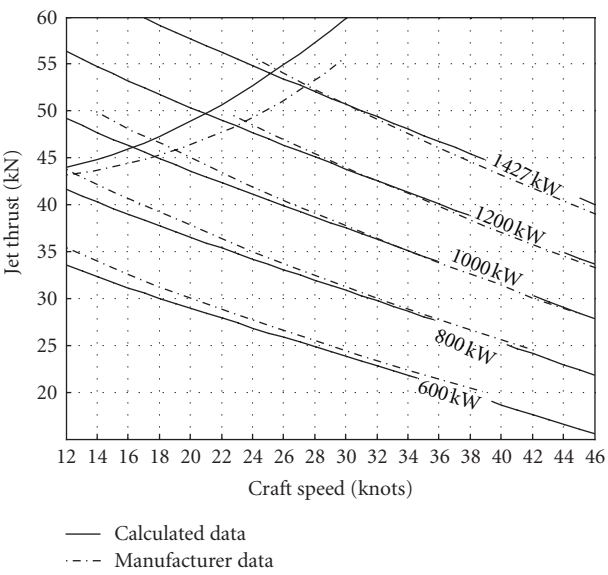

Figure 18: Thrust curves comparison with Hamilton Jet data.

4.2. Case Study 2. The nondimensional waterjets curves are used to reproduce the jet thrust map of a virtual waterjet unit having the same size of two different jet units, produced by Hamilton and MJP. The comparison between the thrust curves (including cavitation limit) calculated by the dimensionless coefficients (solid lines), and the Hamilton manufacturer data (dashed and dotted lines) is reported in Figure 18, while the same kind of comparison, regarding a MJP jet unit, is illustrated again in Figure 19. Calculation is carried out considering an impeller diameter equal to 0.57 m for the comparison with Hamilton waterjet, and an impeller diameter of about 0.6 m for MJP jet unit.

In both applications, the level of accuracy of the proposed numerical procedure is rather good, even if, in the case of MJP waterjet, the results, in terms of jet thrust curves as

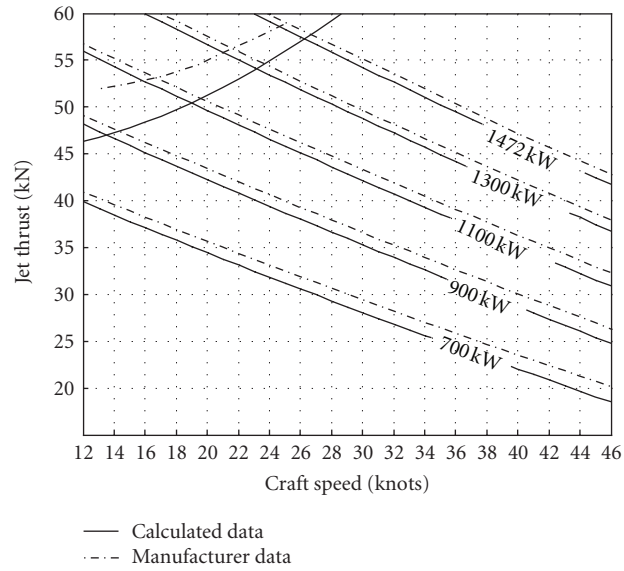

Figure 19: Thrust curves comparison with MJP data.

well as cavitation limit, underestimate the performance in the entire boat speed range. However, it is important to point out that MJP jet units are actually famous for their high performance, while the developed numerical method has been calibrated in order to represent the behavior of most waterjet units, irrespective of the manufacturer.

5. Further Considerations on the Proposed Procedures

The presented procedures have been derived on the ground of many data taken from the most famous waterjets manufactures, then, as a consequence, they are able to reproduce the two main kinds of jet performance prediction, adopted, respectively, for ships applications (e.g., "Kamewa" approach) and for planing craft applications (e.g., "Hamilton Jet" approach). Because of this, the two numerical procedures entail the same levels of approximations adopted by jet manufacturers. From this point of view, the main theoretical difference between the two jet performance approaches, illustrated in Figures 1 and 2, concerns the pump efficiency; it is considered not constant in the representation reported in Figure 1, while it is likely assumed constant for the entire jet working range in Figure 2. In the same way, the first numerical method, based on the use of the dimensionless pump map, is able to consider the pump efficiency variation and then to reproduce the same trend of the jet thrust curve illustrated in Figure 1 and typical of the larger waterjet units (in addition, also the cavitation influence on the decreasing pump efficiency is considered). On the contrary, the second presented method is based on a strong simplification, for which a cubic law relationship of the pump power with the rotational speed is assumed (that means pump efficiency always constant). However, this latter hypothesis is often adopted also in the powering predictions provided by the jet manufacturers for small applications, as it is illustrated

on the right of Figure 2; therefore, the authors have decided to adopt the same design approach in order to compare the obtained results with the data provided by the small jet manufacturers. It is important to point out that, in this case, the jet performance prediction is valid only for subcavitating zone, since no attempt is taken into consideration for evaluating the jet thrust loss due to cavitation. However, despite this significant different assumption in the two representations of the jet data, both numerical methods give approximately the same results in terms of jet final working points for a certain hull resistance; this effect is probably due to the fact that the pump working points, in the steady-state condition, very often lay in the region where the pump efficiency is almost constant.

Both methods offer advantages and drawbacks on the basis of which level of approximation is pursued. The method based on the pump map allows a more reliable final performance prediction in the whole jet working range, but it needs some precise input information, as the pump flow rate, head, speed, and efficiency at the nominal condition for the numerical evaluation of the pump map, the nozzle diameter, the inlet-duct losses, the pump suction specific speed for cavitation influence calculation, and so forth.

On the contrary, the second illustrated procedure may be defined as "parametric," since it is based on simple parameters (mainly the impeller diameter), "traditional," since it uses marine traditional definitions (e.g., thrust and torque coefficients) and finally "computationally-friendly" because it can be easily implemented in numerical codes.

6. Conclusions

The main purpose of this work is to provide the ship designer a reliable tool to be used at early design stage of high-speed craft to facilitate the selection of the propulsion system. To reach this goal in the paper, two original nondimensional approaches, able to foresee the waterjet working points in all of the desired conditions and mainly to take into account the influence of the numerous parameters affecting the waterjet-ship system, are presented and discussed. In particular, the paper describes the hypotheses, the genesis, the tuning, and the application of these general numerical procedures.

The good agreement between waterjets reference data and results obtained by the developed procedures allows to identify the following major findings.

(i) Despite several geometrical differences among the most used impellers for waterjet propulsion, it is shown that the nondimensional standard performance map, derived by the authors for mixed flow pumps, is able to represent with a good level of accuracy the performance predictions of large waterjets of different sizes.

(ii) Similarly, it is demonstrated that it is possible to directly provide the representation of the jet thrust, depending on engine power and craft speed, in a dimensionless form. Then, the second numerical approach, developed by the authors and based on simple and clearly defined parameters, can be useful to represent the performance of a large range of waterjet units for planing boats.

(iii) Although in literature some other studies introduce parametric models for the evaluation of the jet thrust, in the present work, the numerical methods proposed by the authors are able to take into account also cavitation phenomena, on the basis of practical and significant numerical coefficients.

The waterjet units are obviously optimized for each application by the jet manufacturers; however, only the ship/boat designer is responsible for the entire system. In this sense, the two presented calculation methodologies may represent a reliable tool in order to assess the waterjet performance, in terms of jet thrust, power absorption, and cavitation limits, giving in this way a significant contribution to the success of the whole ship design process.

Nomenclature

a:	Exponent to be adopted for the boundary layer expression
A_j:	Waterjet exit area [m^2]
C:	Constant of the cubic law between absorbed jet power and rotational speed
D_i:	Impeller diameter [m]
F_{corr}:	Correction function for pump cavitation
g:	Gravity acceleration [m/s^2]
h:	Waterjet exit nozzle elevation [m]
h_{pi}:	Static head at pump inlet [m]
h_j:	Height of jet centerline above sea level [m]
H:	Pump head [m]
H_{corr}:	Pump head corrected for cavitation [m]
H_d:	Pump design head [m]
J_{wj}:	Waterjet advance coefficient
$K_{Q_{\text{wj}}}$:	Waterjet torque coefficient
$K_{T_{\text{wj}}}$:	Waterjet thrust coefficient
l_i:	Inlet section width [m]
n:	Pump speed [rev/s]
n_d:	Pump design speed [rev/s]
N_{wj}:	Number of jets
NPSH:	Net positive suction head [m]
n_s:	Pump specific speed [rpm m$^{3/4}$ s$^{-1/2}$]
n_{ss}:	Pump suction specific speed
p_a:	Atmospheric pressure [Pa]
p_v:	Vapor pressure [Pa]
P_B:	Pump power demand [kW]
Q:	Pump flow rate [m^3/s]
Q_d:	Pump design flow rate [m^3/s]
Q_{wj}:	Waterjet torque [Nm]
R_T:	Hull resistance [N]
t:	Thrust deduction factor
T_{cav}:	Cavitation thrust limit [N]
T_{wj}:	Waterjet thrust [N]
V:	Ship speed [m/s]
V_a:	Approaching velocity [m/s]
V_j:	Jet velocity [m/s]
α:	Impeller rating
δ:	Boundary layer thickness [m]

ζ: Waterjet duct loss factor
η_m: Mechanical efficiency
η_N: Nozzle efficiency
η_p: Pump efficiency
$\eta_{p\,\mathrm{corr}}$: Pump efficiency corrected for cavitation
η_{pd}: Pump design efficiency
η_r: Relative rotative pump efficiency
ρ: Sea water density [kg/m^3]
σ_{wj}: Waterjet cavitation number
$\tau_{C_{\mathrm{wj}}}$: Waterjet cavitation thrust coefficient.

Acknowledgments

The authors wish to thank Termomeccanica Pompe S.p.A., Rolls Royce Marine Systems (Genova, Italy), Hamilton Jet and MJP for the information kindly provided during the work.

References

[1] P. Hu and M. Zangeneh, "CFD calculation of the flow through a waterjet pump," in *Proceedings of the International Conference on Waterjet Propulsion III*, RINA, Stockholm, Sweden, 2001.

[2] W. G. Park, J. H. Jang, H. H. Chun, and M. C. Kim, "Numerical flow and performance analysis of waterjet propulsion system," *Ocean Engineering*, vol. 32, no. 14-15, pp. 1740–1761, 2005.

[3] N. Bulten and R. Verbeek, "Interpretation of model scale test results with aid of CFD calculations," in *Proceedings of the RINA Waterjet Propulsion III Conference*, Gothenburg, Sweden, 2001.

[4] N. Bulten and R. Verbeek, "Design of optimal inlet duct geometry based on vessel operation profile," in *Proceedings of the 7th International Conference on Fast Sea Transportation (FAST '03)*, Ischia, Italy, 2003.

[5] Y. Qiongfang, W. Yongsheng, Z. Zhihong, and Z. Mingmin, "Research on the optimum blades number of mixed flow pump based on CFD," in *Proceedings of the International Waterjet Propulsion 5 Conference*, pp. 17–26, RINA, London, UK, December 2008.

[6] C. Liu, Y. Wang, and Z. Zhang, "Numerical simulation and analysis of cavitation performance of waterjet," in *Proceedings of the International Waterjet Propulsion 5 Conference*, pp. 59–68, RINA, London, UK, December 2008.

[7] T. Van Terwisga, "The effect of waterjet-hull interaction on thrust and propulsion efficiency," in *Proceedings of the 1st International Conference on Fast Sea Transportation (FAST '91)*, vol. 2, pp. 1149–1167, month year.

[8] T. Van Terwisga, "A parametric propulsion prediction method for waterjet driven craft," in *Proceedings of the 4th International Conference on Fast Sea Transportation (FAST '97)*, Sydney, Australia, 1997.

[9] D. M. MacPherson, "A universal parametric model for waterjet performance," in *Proceedings of the 5th Annual Fast Ship Conference (FAST '99)*, Seattle, Wash, USA, 1999.

[10] J. Allison, "Marine waterjet propulsion," in *Proceedings of the SNAME Annual Meeting*, vol. 101, pp. 275–335, September 1993.

[11] G. Benvenuto, U. Campora, M. Figari, and V. Ruggiero, "A dynamic model for the performance prediction of a waterjet propulsion system," in *Proceedings of the 7th International Symposium on Practical Design of Ships and Mobile Units (PRADS '98)*, The Hague, The Netherlands, September 1998.

[12] G. Benvenuto, M. Figari, and V. Ruggiero, "Waterjet propulsion system performance prediction by dynamic numerical simulation," in *Proceedings of the 5th International Symposium on "High Speed Marine Vehicles (HSMV '99)*, Capri, Italy, March 1999.

[13] M. Altosole, G. Benvenuto, U. Campora, and M. Figari, "Performance prediction of a waterjet propelled craft by dynamic numerical simulation," in *Proceedings of the 4th International Conference of RINA-Waterjet Propulsion*, London, UK, May 2004.

[14] E. Jahanbakhsh, R. Panahi, and M. S. Seif, "Development of numerical tool for hydrodynamic simulation of high speed planing crafts," in *Proceedings of the 6th International Conference on High Speed Marine Vehicles (HSMV '08)*, Naples, Italy, September 2008.

[15] J. E. Buckingham, "Modelling of waterjets in a propulsion system," in *Proceedings of the 4th International Conference of RINA-Waterjet Propulsion*, London, UK, May 2004.

[16] R. Svensson, S. Brizzolara, and L. Grossi, "Trial result including wake measurements from the world's largest waterjet installation," in *Proceedings of the International Conference on Waterjet Propulsion-Latest Developments*, Amsterdam, The Netherlands, October 1998.

[17] S. L. Dixon, *Fluid Mechanics, Thermodynamics of Turbomachinery*, Pergamon Press Book Company, Oxford, UK, 1st edition, 1966.

[18] M. Sedille, *Turbo-Machines Hidrauliques et Thermiques, Tome II-Pompes Centrifugues et Axialles, Turbines Hidrauliques*, Masson Ed, Paris, France, 1967.

[19] I. J. Karassik and W. C. Krutzsch, *Centrifugal and Axial Pumps, Marks' Standard Handbook for Mechanical Engineers*, McGraw-Hill Book Company, New York, NY, USA, 8th edition, 1981.

[20] G. Benvenuto and U. Camporaes, "A generalized mixed flow pump model for waterjets simulation," in *Proceedings of the World Maritime Technology Conference*, London, UK, 2006.

[21] http://www.fpipumps.com/, FPI Internet address, 2004.

[22] S. Lipani, *Performance characteristics maps of the pumps employed in the waterjet propulsion [Engineer Degree Thesis]*, Department of Naval Engineer & Marine Technology and Department of Fluid Machinery, Energy Systems and Transportation, University of Genova, Genova, Italy, 2004.

[23] TM.P. Termomeccanica Pumps, "Termomeccanica pompe," Tech. Rep., TM.P. Termomeccanica Pumps, La Spezia, Italy, 2004.

[24] M. Altosole, G. Benvenuto, and M. Figari, "Waterjet performance prediction," in *Proceedings of the International Conference on Ship and Shipping Research (NAV '03)*, Palermo, Italy, June 2003.

[25] A. Keith, "Waterjet versus propeller engine matching characteristics," *Naval Engineers Journal*, vol. 107, no. 3, pp. 129–139, 1995.